Differential bottomonium observables from quantum trajectories

Quark Confinement and the Hadron Spectrum 2021

Peter Vander Griend

based on JHEP 05 (2021) 136 and arXiv:2107.06222

in collaboration with Nora Brambilla, Miguel Escobedo, Michael Strickland, Antonio Vairo, and Johannes Weber

Technical University of Munich

6 August 2021

Introduction

Motivation: use heavy quarks and their bound states to probe the strongly coupled medium formed in heavy ion collisions

- high mass M of bottom quarks and the short formation time of their bound states make them ideal probes of the quark gluon plasma (QGP); observables of interest include nuclear suppression factor R_{AA} and elliptic flow v_2
- ideally suited for treatment using the formalism of open quantum systems (OQS) and effective field theory (EFT)
  - OQS: allows for the rigorous treatment of a quantum system of interest (heavy quarkonium) coupled to an environment (QGP)
  - EFTs: take advantage of the large mass of the heavy quark and the resulting nonrelativistic nature of the system and small bound state radius using potential nonrelativistic QCD (pNRQCD), an EFT of the strong interaction

Advantages: fully quantum, non-Abelian, heavy quark number conserving, account for dissociation and recombination, and valid for strong or weak coupling

potential Non-Relativistic QCD (pNRQCD)

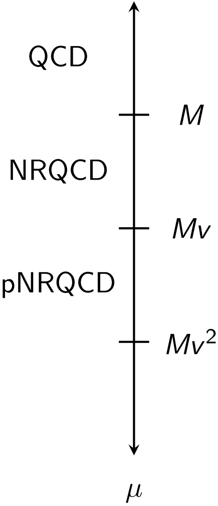

- effective theory of the strong interaction obtained from full QCD via non-relativistic QCD (NRQCD) by successive integrating out of the hard (M) and soft (Mv) scales where $v \ll 1$ is the relative velocity in a heavy-heavy bound state
- degrees of freedom are singlet and octet heavy-heavy bound states and ultrasoft gluons
- small bound state radius and large quark mass allow for double expansion in r and M^{-1} at the Lagrangian level

Hierarchies and Simplifying Assumptions

quantum Brownian motion

for

$$\tau_R, \tau_S \gg \tau_E,$$

where τ_R, τ_S, and τ_E are the relaxation, system intrinsic, and environment correlation time scales, respectively, the system realizes **quantum Brownian motion**

Simplifying Approximations

hierarchy of scales allows for two simplifying approximations:

- **Born approximation**: quarkonium has little effect on the medium at time scales of interest; density matrix factorizes, i.e., $\rho(t) \propto \rho_S(t) \otimes \rho_E$
- **Markov approximation**: only the state of the quarkonium at the present time is necessary to describe its evolution, i.e., no memory integral

Physical Setup

relevant energy scales (EFT)

- heavy quark mass $M = M_b \sim 5$ GeV
- inverse Bohr radius $1/a_0 \sim 1.5$ GeV
- (π times) the temperature of the medium $(\pi)T \sim 1.5$ GeV
- (Coulombic) binding energy $E \sim 0.5$ GeV
- hierarchical ordering: $M,\ 1/a_0 \gg (\pi)T \gg E$ [1]

relevant time scales (OQS)

- system intrinsic time scale: $\tau_S \sim 1/E$
- environment correlation time: $\tau_E \sim 1/(\pi T)$
- relaxation time: $\tau_R \sim 1/\Sigma_s \sim 1/(a_0^2(\pi T)^3)$ (where Σ_s is the thermal self energy)

---

[1] $\pi T \sim 1.5$ GeV at initial time; medium quickly expands and cools such that $1/a_0 \gg \pi T$ is realized

Evolution Equations of in Medium Coulombic Quarkonium[2]

$$\frac{\mathrm{d}\rho_s(t)}{\mathrm{d}t} = -\,i\,[h_s, \rho_s(t)] - \Sigma_s \rho_s(t) - \rho_s(t)\Sigma_s^\dagger + \Xi_{so}(\rho_o(t)),$$
$$\frac{\mathrm{d}\rho_o(t)}{\mathrm{d}t} = -\,i\,[h_o, \rho_o(t)] - \Sigma_o \rho_o(t) - \rho_o(t)\Sigma_o^\dagger + \Xi_{os}(\rho_s(t)) + \Xi_{oo}(\rho_o(t))$$

- $\rho_{s,o}(t)$: density matrix of color singlet, octet bound state
- $h_{s,o} = \frac{\mathrm{p}^2}{M} + V_{s,o}$: singlet, octet Hamiltonian
  - $V_s = -\frac{C_f \alpha_s(1/a0)}{r}$: singlet potential
  - $V_o = \frac{\alpha_s(1/a0)}{2N_c r}$: octet potential
- Σ, Ξ: encode medium interactions in correlators of the form

$$\Sigma,\ \Xi \sim \langle \tilde{E}^{a,j}(0,\mathbf{0})\tilde{E}^{a,j}(s,\mathbf{0})\rangle, \quad \tilde{E}^{a,i}(s,\mathbf{0}) = \Omega(s)E^{a,i}(s,\mathbf{0})\Omega(s)^\dagger,$$

$$\Omega(s) = \exp\left[-ig\int_{-\infty}^{s} \mathrm{d}s' A_0(s',\mathbf{0})\right]$$

[2] Phys. Rev. D 97, 074009 (2018).

Master Equation

evolution equations can be rewritten as master equation

$$\frac{\mathrm{d}\rho(t)}{\mathrm{d}t} = -i[H,\rho(t)] + \sum_{n,m} h_{nm}\left(L_i^n\rho(t)L_i^{m\dagger} - \frac{1}{2}\left\{L_i^{m\dagger}L_i^n,\rho(t)\right\}\right),$$

where

$$\rho(t) = \begin{pmatrix} \rho_s(t) & 0 \\ 0 & \rho_o(t) \end{pmatrix}, \quad H = \begin{pmatrix} h_s + \mathrm{Im}(\Sigma_s) & 0 \\ 0 & h_o + \mathrm{Im}(\Sigma_o) \end{pmatrix},$$

$$L_i^0 = \begin{pmatrix} 0 & 0 \\ 0 & 1 \end{pmatrix} r^i, \quad L_i^1 = \begin{pmatrix} 0 & 0 \\ 0 & \frac{N_c^2-4}{2(N_c^2-1)}A_i^{oo\dagger} \end{pmatrix}, \quad L_i^2 = \begin{pmatrix} 0 & \frac{1}{\sqrt{N_c^2-1}} \\ 1 & 0 \end{pmatrix} r^i,$$

$$L_i^3 = \begin{pmatrix} 0 & \frac{1}{\sqrt{N_c^2-1}}A_i^{os\dagger} \\ A_i^{so\dagger} & 0 \end{pmatrix}, \quad h = \begin{pmatrix} 0 & 1 & 0 & 0 \\ 1 & 0 & 0 & 0 \\ 0 & 0 & 0 & 1 \\ 0 & 0 & 1 & 0 \end{pmatrix},$$

$$\boxed{A_i^{uv} = \frac{g^2}{6N_c}\int_0^\infty \mathrm{d}s\, e^{-ih_u s} r^i e^{ih_v s}\langle \tilde{E}^{a,j}(0,\mathbf{0})\tilde{E}^{a,j}(s,\mathbf{0})\rangle}$$

Lindblad Equation

- for $(\pi)T \gg E$, $e^{-ih_{s,o}s} \approx 1$ and medium interactions simplify

$$A_i^{uv} = \frac{r^i}{2}(\kappa - i\gamma),$$

where

$$\kappa = \frac{g^2}{6N_c}\int_0^\infty \mathrm{d}t \left\langle \left\{ \tilde{E}^{a,i}(t,0), \tilde{E}^{a,i}(0,0) \right\} \right\rangle,$$
$$\gamma = -\frac{ig^2}{6N_c}\int_0^\infty \mathrm{d}t \left\langle \left[\tilde{E}^{a,i}(t,0), \tilde{E}^{a,i}(0,0) \right] \right\rangle$$

- κ is the heavy quark momentum diffusion coefficient; γ is its dispersive counterpart
- evolution equation can be written as Lindblad equation

$$\frac{\mathrm{d}\rho(t)}{\mathrm{d}t} = -i[H(t),\rho] + \sum_n \left(C_i^n \rho(t) C_i^{n\dagger} - \frac{1}{2}\left\{ C_i^{n\dagger} C_i^n, \rho(t) \right\} \right)$$

Transport Coefficients

- κ is the heavy quark momentum diffusion coefficient; γ is its dispersive counterpart
- κ and γ related to in-medium width and mass shift of $\Upsilon(1S)$:

$$\Gamma(1S) = 3a_0^2\kappa, \quad \delta M(1S) = \frac{3}{2}a_0^2\gamma,$$

  and accessible from unquenched lattice measurements of Γ and δM
- temperature dependent $\kappa(T)$ measured directly in quenched lattice simulations

Extraction of Transport Coefficients

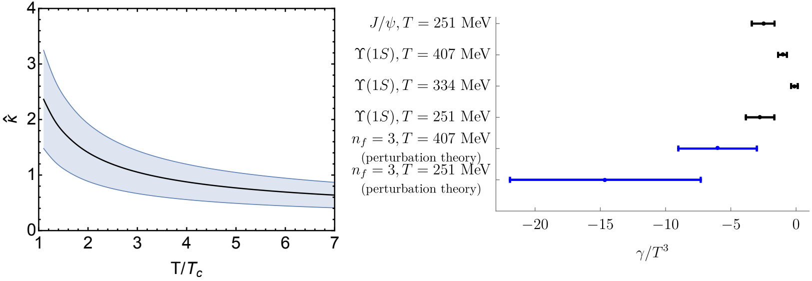

Figure: (Left) Direct, quenched lattice measurement of $\hat{\kappa} = \kappa/T^3$ (Phys. Rev. D 102, 074503 (2020)). (Right) Indirect extractions of $\hat{\gamma} = \gamma/T^3$ from unquenched lattice measurements of $\delta M(1S)$ (lattice extractions of $\delta M(1S)$ from JHEP 11 (2018) 088 and Phys.Rev.D 100 (2019) 7, 074506).

We solve the Lindlbad equation using the upper, central, and lower $\hat{\kappa}(T) = \kappa(T)/T^3$ curves and $\hat{\gamma} = \gamma/T^3 = \{-3.5, -1.75, 0\}$.

Quantum Trajectories Algorithm

- computationally more efficient to work with wave function $|\psi\rangle$ than density matrix ρ
- absorb quantum number conserving diagonal evolution terms of Lindblad equation into a non-Hermitian effective Hamiltonian

$$H_{eff} = H - \frac{i}{2}\sum_n C_n^\dagger C_n$$

- evolve deterministically with H_{eff}

$$|\psi(t)\rangle = e^{-i\int_{t_0}^{t} dt' H_{\text{eff}}(t')}|\psi(t_0)\rangle$$

- evolution with H_{eff} reduces norm; norm at time t related to probability that a change of quantum numbers occurs
- Monte Carlo sample to determine change of quantum numbers and implement by applicating collapse operator, i.e., $C_n|\psi(t)\rangle$
- we developed the `QTraj` code implementing the quantum trajectories algorithm for the Lindblad equation describing the time evolution of heavy quarkonium in a strongly coupled plasma[3]

[3] arXiv:2107.06147

QTraj Implementation

1. initialize wave function $|\psi(t_0)\rangle$
2. generate random number $0 < r_1 < 1$, evolve with H_{eff} until

$$|| \, e^{-i \int_{t_0}^{t} dt' H_{\text{eff}}(t')} |\psi(t_0)\rangle \, ||^2 \leq r_1,$$

   and initiate a quantum jump
3. quantum jump
   - 3.1 if singlet, jump to octet; if octet, generate random number $0 < r_2 < 1$ and jump to singlet if $r_2 < 2/7$; otherwise, remain in octet
   - 3.2 generate random number $0 < r_3 < 1$; if $r_3 < l/(2l+1)$, $l \to l-1$; otherwise, $l \to l+1$.
   - 3.3 multiply wavefunction by r and normalize
4. Continue from step 2.

each realization of the above algorithm is a *quantum trajectory*; the average of N trajectories tends toward the solution of the Lindblad equation as $N \to \infty$

Simulation Parameters

- Gaussian-smeared delta initial condition:
  $\psi_\ell(t_0) \propto r^\ell e^{-r^2/(ca_0)^2}$; width $c = 0.2$
- `NUM`$=$4096 spatial lattice sites, radial volume `L`$= 80$ GeV^{-1}, lattice spacing $a \approx 0.0195$ GeV^{-1}, temporal discretization `dt`$= 0.001$ GeV^{-1}
- approximately $7 - 9 \times 10^5$ physical trajectories allowing for extraction of differential observables including v_2 and results as a function of transverse momentum p_T
- 50-100 quantum trajectories per physical trajectory
- vacuum evolution from initialization at $t_0 = 0$ fm until initialization of interaction with medium at $t = 0.6$ fm and vacuum evolution for $T < T_f = 250$ MeV

R_{AA} vs. p_T

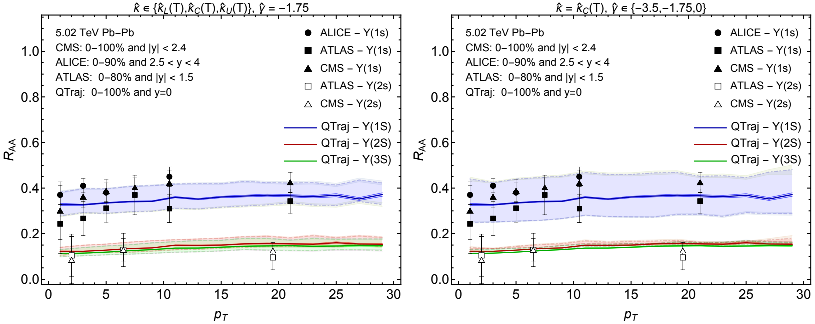

Figure: The nuclear modification factor R_{AA} of the $\Upsilon(1S)$, $\Upsilon(2S)$, $\Upsilon(3S)$ as a function of p_T compared to experimental measurements. The bands in the left plot represent variation of $\hat{\kappa}$ at fixed $\hat{\gamma} = -1.75$; the bands in the right plot represent variation of $\hat{\gamma}$ at fixed $\hat{\kappa} = \hat{\kappa}_C$.

Double Ratio $2S$ vs. p_T

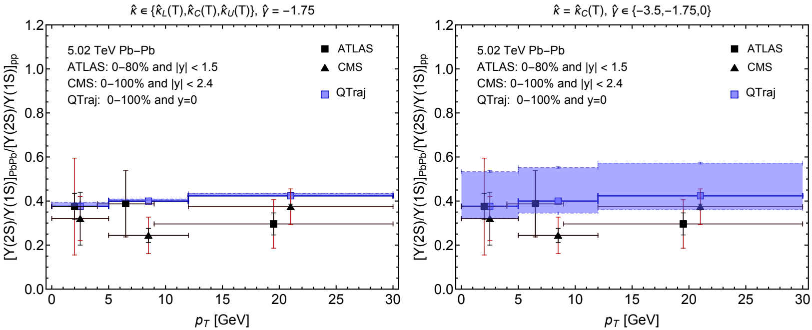

Figure: The double ratio of the nuclear modification factor $R_{AA}[\Upsilon(2S)]$ to $R_{AA}[\Upsilon(1S)]$ as a function of p_T compared to experimental measurements. The bands in the left plot represent variation of $\hat{\kappa}$ at fixed $\hat{\gamma} = -1.75$; the bands in the right plot represent variation of $\hat{\gamma}$ at fixed $\hat{\kappa} = \hat{\kappa}_C$. The black and red bars in the experimental data represent statistical and systematic uncertainties, respectively.

$v_2[\Upsilon(1S)]$ vs. Centrality

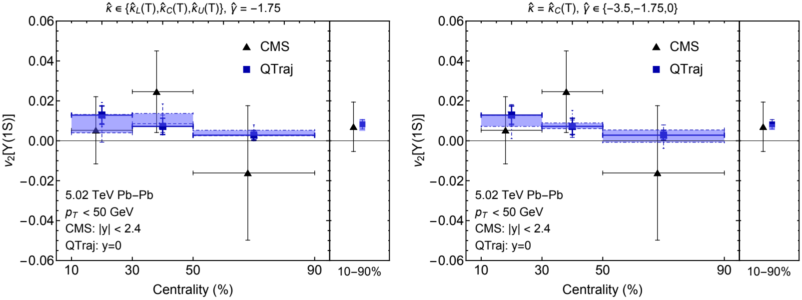

Figure: The elliptic flow v_2 of the $\Upsilon(1S)$ as a function of centrality compared to experimental measurements. The bands in the left plot represent variation of $\hat{\kappa}$ at fixed $\hat{\gamma} = -1.75$; the bands in the right plot represent variation of $\hat{\gamma}$ at fixed $\hat{\kappa} = \hat{\kappa}_C$.

$v_2[\Upsilon(1S)]$ vs. p_T

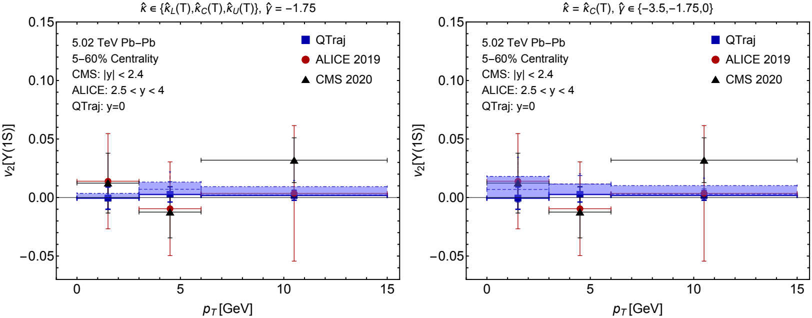

Figure: The elliptic flow v_2 of the $\Upsilon(1S)$ as a function of p_T compared to experimental measurements. The bands in the left plot represent variation of $\hat{\kappa}$ at fixed $\hat{\gamma} = -1.75$; the bands in the right plot represent variation of $\hat{\gamma}$ at fixed $\hat{\kappa} = \hat{\kappa}_C$.

$v_2[\Upsilon(2,3S)]$ vs. Centrality

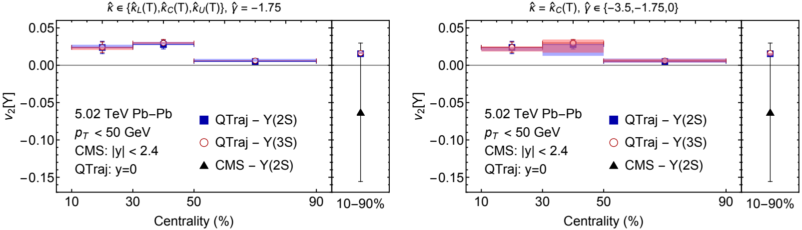

Figure: The elliptic flow v_2 of the $\Upsilon(2S)$ and $\Upsilon(3S)$ as a function of centrality compared to experimental measurements. The bands in the left plot represent variation of $\hat{\kappa}$ at fixed $\hat{\gamma} = -1.75$; the bands in the right plot represent variation of $\hat{\gamma}$ at fixed $\hat{\kappa} = \hat{\kappa}_C$.

Experimental References

Plot	Reference (Experiment)
R_{AA} vs. p_T	arXiv:2011.05758 (ALICE) link to presentation (ATLAS) Phys. Lett. B 790 (2019) 270 (CMS)
Double Ratio 2S vs. p_T	link to presentation (ATLAS) Phys. Rev. Lett. 120, 142301 (2018) (CMS)
$v_2[\Upsilon(1S)]$ vs. Centrality	Phys. Lett. B 819 (2021) 136385 (CMS)
$v_2[\Upsilon(1S)]$ vs. p_T	Phys. Rev. Lett. 123, 192301 (2019) (ATLAS) Phys. Lett. B 819 (2021) 136385 (CMS)
$v_2[\Upsilon(2,3S)]$ vs. p_T	Phys. Lett. B 819 (2021) 136385 (CMS)

Conclusions and Outlook

- scale hierarchy makes heavy quarkonia excellent probes of the quark gluon plasma formed in heavy ion collisions; observables of interest include nuclear modification factor R_{AA} and elliptic flow v_2
- computational methods necessary to calculate R_{AA} and v_2
- `QTraj` implements the quantum trajectories algorithm to solve the Lindblad equation and extract R_{AA} and v_2 as functions of centrality and transverse momentum
- results show good agreement with experimental data
- method and results are fully quantum, non abelian, and heavy quark number conserving; take into account dissociation and recombination; and depend only on the transport coefficients κ and γ the values of which we take from lattice data